JOURNAL OF MATERIALS SCIENCE 20 (1985) 482–490

The effect of grinding on the flexural strength of a sialon ceramic

M. W. HAWMAN*, P. H. COHEN†, J. C. CONWAY, R. N. PANGBORN
Department of Engineering Science and Mechanics, and †Industrial and Management Systems Engineering, The Pennsylvania State University, University Park, PA 16802, U.S.A.

The effect of selected grinding parameters on the flexural strength of a sialon ceramic was studied. Support compliance was found to have no significant effect, while depth of incursion and grinding direction did. Weibull statistics and analysis of variance techniques were used to detect these effects which are explained through flaw magnitude and direction.

1. Introduction

Grinding treatments are commonly used to fabricate ceramic parts to close tolerances. Although grinding produces the desired dimensions, machining-induced surface flaws can significantly reduce the strength and performance of the material. The purpose of this investigation was to evaluate the effects of selected grinding parameters on the flexural strength of a sialon ceramic.

Sialon ceramics have great potential for high temperature and high stress applications such as cutting tools, turbine blades, and bearings [1]. Since these components will require various machining operations during their manufacture, it is important to understand the effect of surface grinding on this ceramic.

It is well known that grinding variables can have a significant impact on the flexural strength of alumina, silicon nitride, and glass [2–5]. The effect of grinding variables such as depth of incursion, grit size, feed rate, and feed direction have been studied. The predominant trend identified through these investigations is that flexural strength decreases when either material removal rates or grit size are increased [2, 3]. Additionally, flexural strengths measured parallel to the grinding direction have been found to be greater in magnitude than those measured perpendicular to the grinding direction [3]. This phenomenon has been explained in analytical investigations which predict more severe subsurface planar flaw generation parallel to the grinding direction [5].

In this investigation, the grinding variables chosen for study were depth of incursion, grinding direction with respect to the length of the flexural specimen, and support compliance during grinding. The effect of the depth of incursion was evaluated by flexural tests conducted on beam specimens having 0.003 in. (0.076 mm) of material removed in either a single grinding pass, or in six consecutive passes with a 0.0005 in. (0.013 mm) thick layer removed on each pass. In each case, grinding was performed both parallel and perpendicular to the length of the flexural specimen. The effect of support compliance was evaluated by comparing flexural test results for specimens mechanically clamped to the grinding table with the data for specimens secured by Rigidax wax.‡ Groenou *et al.* [6] have shown that the grinding force is pulsed at a frequency equal to that of the grinding wheel so that vibrations are introduced into the workpiece. The more compliant Rigidax support was therefore adopted to possibly dampen these vibrations which could affect the amount of surface damage done to the ceramic.

2. Experimental procedures

2.1. Experimental design

For this initial study, three possible parameters of importance were selected; depth of incursion,

*Present address: United Technologies Research Center, East Hartford, Connecticut, USA.
‡Rigidax Tooling Compound, M. Argueso & Co Inc, 441, Waverly Avenue, Mamaroneck, NY, USA.

0022–2461/85 $03.00 + .12

grinding direction, and support compliance. With little *a priori* information and the intent also to evaluate the interactive effects of these variables, a 2^3 full factorial experimental design was chosen. Eighteen replications were conducted due to the wide dispersion normally associated with the flexural strength of brittle materials. In addition, Weibull statistics were used to characterize the strength-controlling flaw populations for each treatment combination.

2.2. Grinding equipment

Grinding was performed on a Brown and Sharpe surface grinder incorporating a 600-grit resin-bonded diamond grinding wheel. The six-inch diameter wheel was operated at 3200 rpm with a continuous spray application of a water-soluble, oil coolant/lubricant with a 40:1 ratio of water to oil. Up-grinding was used with a table feed of 10.2 in. min^{-1} (25.8 cm min^{-1}).

A Kistler model 9273 piezoelectric dynamometer preamplified using a Kistler Type 5001 amplifier and connected to a Nicolet model 2090-111A digital oscilloscope was used to record the loads on the workpiece during grinding. Horizontal and vertical forces during grinding were displayed on the oscilloscope and their peak values determined from their respective traces.

2.3. Specimen preparation

The as-sintered sialon beams measured 0.225 in. × 0.225 in. × 0.800 in. (5.7 mm × 5.7 mm × 21 mm). The reaction layer from sintering was removed from the test surface of each beam by up-grinding along the beam's length. A total of 0.008 in. (0.203 mm) of material was removed in sixteen consecutive passes of 0.0005 in. (0.013 mm) incursion depth. The remaining three sides of the sialon beams were prepared in a similar manner except back-and-forth grinding was used for expediency. After final grinding of the test surface, the edges adjacent to this surface were chamfered manually using 600-grit wet abrasive paper. This precaution was taken to reduce the number of failures initiated at edge flaws, an occurrence often reported in previous investigations [2].

2.4. Flexural testing

A test fixture, designed to incorporate both three- and four-point bend configurations, is shown in Fig. 1. The loading heads were self-adjusting to slight imperfections in the beam specimen's shape. The lower specimen supports consisted of two ball bearings pressed into the lower base plate. The upper loading head swivelled on a cylinder secured to the upper base plate. A single dowel pin, in the case of three-point bend, and two dowel pins, in the case of four-point bend, were attached to the upper loading head to contact the beam specimen. The lower base plate was attached to the load-cell train of the Instron testing machine while the upper base plate was attached to the cross-head. This configuration allowed the Instron to be operated in a tensile mode, thus preventing the weight of the fixture from contributing to the applied load.

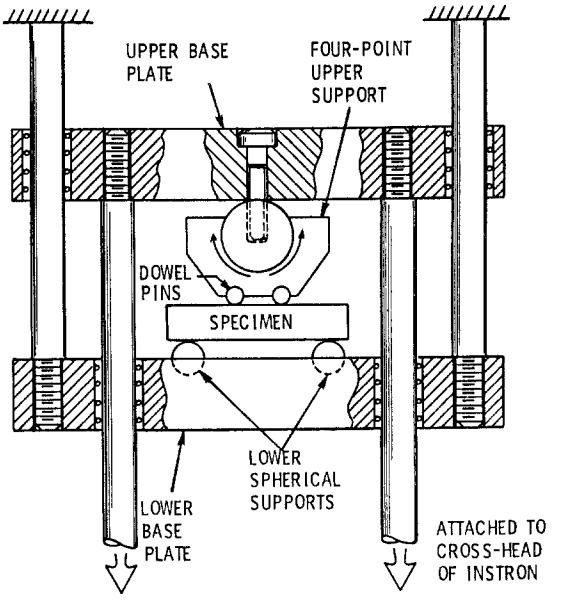

Figure 1 Specimen loading fixture configured in four-point bend.

The ASTM specifications for measuring the flexural modulus of brittle materials vary widely with respect to specimen dimensions and test configuration. For example, ceramic whiteware requires three-point bend with a 4.5 in. (11.4 cm) beam length while 10 in. (25.4 cm) long specimens of glass are tested in four-point bend. The closest ASTM specification to the material and specimen dimensions used in this investigation is for cemented carbide [7]. This specification requires that 0.75 in. (1.9 cm) beams be tested in three-point bend and failure must occur within the middle third of the beam for a test to be acceptable. Since a bending moment gradient is produced along the beam's length, this would allow the

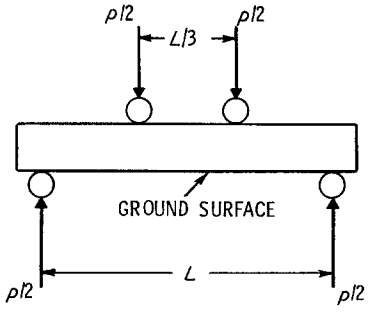

Figure 2 Diagram of a beam-specimen in four-point bend.

actual failure stress to be as much as 33% lower than that determined assuming mid-span fracture. Additionally, the abrupt change in sign of the vertical shear force at mid-span in three-point bend may also introduce undesirable effects.

In contrast, four-point bend develops a constant bending moment in the region between the inner load points without the presence of any transverse shear force. To eliminate the possibility of crushing the beam specimen between adjacent upper and lower load points, the spacing between the inner supports was set at one-third of the outer support distance as shown in Fig. 2. A photoelastic model of the sialon beam was used to confirm that a suitable stress distribution was generated in four-point bend. The dark-field photograph, in Fig. 3, shows the constant stress region along the lower surface between the upper load points. Provided that failure does originate at the surface in this region, the fracture stress can be simply computed by measuring the applied load.

Based on these considerations, four-point bend was chosen as the appropriate test configuration for this investigation. The outer supports were spaced 0.625 in. (1.6 cm) apart with the inner points located at intervals of one-third of the lower support spacing. The beam specimens were loaded to failure at a constant cross-head speed of 0.02 in. min^{-1} (0.51 mm min^{-1}) while applied loads were recorded autographically.

3. Experimental results

3.1. Grinding forces

For a 0.003 in. (0.076 mm) depth of incursion, peak vertical forces averaged 136 lbf $in.^{-1}$ (237 N cm^{-1}) while peak horizontal forces averaged 31 lbf $in.^{-1}$ (55 N cm^{-1}) during grinding. For the smaller 0.0005 in. (0.013 mm) incursion depth, the peak vertical force averaged 56 lbf $in.^{-1}$ (98 N cm^{-1}) while the horizontal force was undetectable within the signal noise. There was no systematic difference between the force traces recorded for the two support compliances for either grinding depth.

3.2. Flexural test results

The mean failure stress and coefficient of variation for each treatment combination is shown in Table I. An analysis of variance was conducted on this data to determine whether any of the grinding variables had an effect on the flexural strength of the sialon beams. The results of the analysis, presented in Table II, show that grinding depth, direction, and the depth–direction interaction to be highly significant. The third parameter, compliance, and the remaining interactions are not significant.

Orthogonal comparisons of the treatment combinations allowed the influence of specific variable levels to be analysed. The results of these comparisons, shown in Table III, show the effect of grinding depth to be significant for the perpendicular grinding direction only. Grinding direction is influential for a 0.003 in. (0.076 mm) depth of cut. Shallow grinding depths of 0.0005 in. (0.013 mm) produce specimens which are insensitive to grinding direction.

Since the relative compliance did not have a measurable effect on the data, the distinction between the support compliances was disregarded and the data combined into the four treatment combinations shown in Table IV. These four data sets were used in the following Weibull statistical analysis.

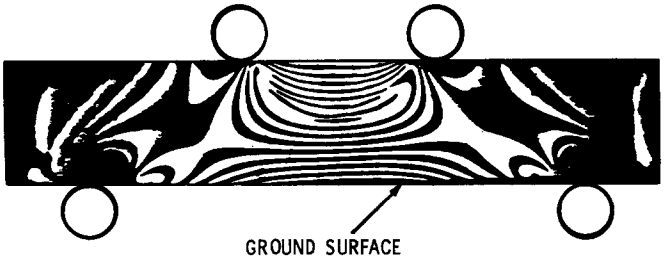

Figure 3 Dark-field photograph of a photoelastic model beam in four-point bend.

TABLE I Mean flexural strength and coefficient of variation for each grinding treatment combination

No. of passes	Depth per pass	Clamped, σ_f		Rigidax, σ_f	
		Parallel	Perpendicular	Parallel	Perpendicular
6	0.0005 in. (0.013 mm)	102 129 p.s.i. (704 MPa) C.V.* = 8.86	95 977 p.s.i. (662 MPa) C.V. = 8.33	97 328 p.s.i. (671 MPa) C.V. = 11.05	98 583 p.s.i. (680 MPa) C.V. = 10.83
1	0.003 in. (0.076 mm)	97 692 p.s.i. (674 MPa) C.V. = 7.66	76 234 p.s.i. (526 MPa) C.V. = 15.98	104 275 p.s.i. (719 MPa) C.V. = 5.32	82 814 p.s.i. (571 MPa) C.V. = 14.83

*Coefficient of variation = (standard deviation/mean) × 100.

3.3. Weibull statistical analysis

Weibull statistics have been used successfully to describe the statistical distributions of the strengths of ceramics. A three-parameter form is generally reduced to a two-parameter form by assuming the lowest possible failure stress to be zero. For failures originating at the specimen's surface, this distribution has the following form:

$$F = 1 - \exp\left[-S(\sigma_f/\sigma_0)^m\right] \quad (1)$$

where F is the cumulative probability of failure, S is the surface area subjected to a uniform bending stress, σ_f is the observed failure stress, σ_0 is a scaling parameter, and m is the Weibull modulus, which is a measure of the variability of the failure stress distribution.

The two Weibull parameters can be obtained from a linearized form of Equation 1:

$$\ln\left[\ln\left(\frac{1}{1-F}\right)\right] = m \ln \sigma_F + [\ln S - m \ln \sigma_0] \quad (2)$$

The result is the equation of a straight line from which the slope provides m, while the scaling parameter is calculated from the intercept.

The method of least-squares was used to fit a straight line to the experimental data for each treatment combination in Table IV. A typical plot is shown in Fig. 4. The correlation coefficients exceeded 0.984 in each case and are shown along with the computed Weibull parameters in Table V. The smallest variability, as evidenced by the largest modulus, m, occurs for the single 0.003 in. (0.076 mm) grinding pass parallel to the length dimension of the beam, while specimens ground with the same incursion depth perpendicular to the length dimension exhibit the largest variability. In contrast, the Weibull modulus shows no directional sensitivity for beams ground with a 0.005 in. (0.013 mm) depth of incursion.

3.4. Ground surface evaluation

The two levels of the incursion depth used in this study were chosen to encompass the range from very light multi-pass grinding to severe single pass grinding conditions. One would expect different surface topography between these extremes due to the amount of heat generation and subsequent flow of the surface material. Fig. 5 shows a scanning electron micrograph of the ground surface for each of the two grinding depths. The substantial amount of heat generated during the deeper 0.003 in. (0.076 mm) grinding, resulted in a smeared surface often characteristic of a material flow process. In contrast, the pitted and cracked surface for the 0.0005 in. (0.013 mm) grinding

TABLE II Analysis of variance for flexural strength

Source	Degrees of freedom	ANOVA sum of squares	F-value	Level of significance
Depth	1	2.35×10^9	24.85	0.0001
Direction	1	4.50×10^9	47.52	0.0001
Compliance	1	2.35×10^8	2.48	0.1174
Depth–compliance	1	4.21×10^8	4.46	0.0367
Direction–compliance	1	1.58×10^8	1.67	0.1985
Depth–direction	1	3.03×10^9	32.03	0.0001
Depth–direction–compliance	1	1.45×10^8	1.53	0.2180
Error	127	1.20×10^{10}	–	–

TABLE III Orthogonal comparisons

Comparison	F-value	Level of significance
Effect of depth on the perpendicular grinding direction	118.06	0.0001
Effect of depth on parallel grinding direction	4.51	0.042
Effect of direction on 0.0005 in. (0.013 mm) incursion depth	1.21	0.262
Effect of direction on 0.003 in. (0.076 mm) incursion depth	99.33	0.0001

depth is more consistent with a cutting or chipping action.

4. Discussion

4.1. Grinding flaws

Rice and Mecholsky [8] have shown that a particle abrading a ceramic surface results in two predominant sets of flaws: one population oriented parallel to the grinding direction and the second oriented perpendicular as shown in Fig. 6. Furthermore, these investigators have shown that the parallel flaws are longer and deeper than those flaws oriented perpendicular to the grinding groove. Conway and Kirchner [9] have correlated this flaw-shape anisotropy to the ratio of horizontal to vertical load during grinding. Analytical results indicated that an increase in the horizontal force component results in an increase in the depth of flaws generated parallel to the grinding direction and has no effect on the depth of flaws generated perpendicular to the grinding direction. Analytical results were experimentally verified.

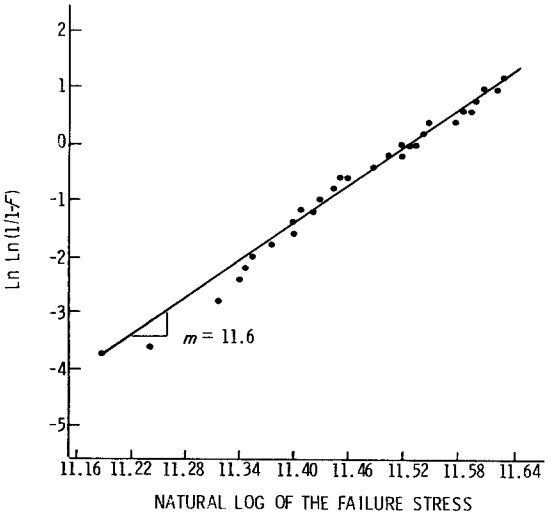

Figure 4 Typical Weibull plot of experimental failure data for six 0.0005 in. (0.013 mm) grinding passes perpendicular to the beams' length dimension.

TABLE IV Flexural strength data for combined compliances

No. of passes	Depth per pass	Grinding direction	
		Parallel	Perpendicular
6	0.0005 in. (0.013 mm)	99 797 p.s.i. (688 MPa) C.V. = 10.08 $n^* = 35$	97 243 p.s.i. (671 MPa) C.V. = 9.62 $n = 35$
1	0.003 in. (0.076 mm)	100 684 p.s.i. (694 MPa) C.V. = 7.32 $n = 33$	79 318 p.s.i. (547 MPa) C.V. = 15.74 $n = 32$

*n = number of specimens.

The orientation of the grinding with respect to the direction of the applied stress will determine which flaw population will be activated during flexural testing. Provided that grinding flaws are the failure origins, a strength anisotropy would be expected since one flaw population is deeper. In this investigation, testing of beams ground perpendicular to their length dimension would activate the deeper flaws induced along the grinding direction, resulting in a lower flexural strength. The possibility that this strength decrease is caused by the stress intensity associated with the grinding grooves has been addressed by Andersson and Bratton [3]. Using a fracture mechanics approach, they have shown that the effect of the grinding groove on the stress intensity is minimal when the crack length is greater than the groove radius.

4.2. Single-pass grinding

The data in Table IV for the 0.003 in. (0.076 mm) grinding depth exhibit the expected strength anisotropy. The analysis of variance and the orthogonal comparisons confirm that there is a statistically significant difference between the flexural strengths for the two grinding directions. The deeper flaws oriented parallel to the grinding direction caused the transversely ground specimens to be 21% weaker in flexure than those beams ground parallel to their length dimension. The theory of Conway and Kirchner predicts that the transversely ground beams should be only 2.3% weaker in flexure, based on the experimentally observed horizontal-

TABLE V Weibull parameters determined from experimental data

No. of passes	Depth per pass	Grinding direction	
		Parallel	Perpendicular
6	0.0005 in. (0.013 mm)	m^* = 11.0 $\sigma_0^\dagger$ = 104 292 p.s.i. (719 MPa) $r^\ddagger$ = 0.984	m = 11.6 σ_0 = 101 411 p.s.i. (699 (MPa) r = 0.992
1	0.003 in. (0.076 mm)	m = 15.2 σ_0 = 104 040 p.s.i. (718 MPa) r = 0.987	m = 6.9 σ_0 = 84 704 p.s.i. (584 MPa) r = 0.989

*m = Weibull modulus.
†σ_0 = scaling parameter.
‡r = correlation coefficient for straight-line fit.

to-vertical load ratio of 0.23. The discrepancy may be attributed to the extension of the analytical theory for single-point grinding to a multi-point grinding situation. Further complications arise from the large amount of material being removed by a grinding wheel with a very fine grit size. The flow of the surface material might significantly alter the force ratio acting on a single grit. Nonetheless, the mechanism by which the horizontal force acts to deepen the longitudinal flaws appears to be valid.

The Weibull parameters for the single-pass grinding data confirm that the critical flaw populations for the two grinding directions are distinct

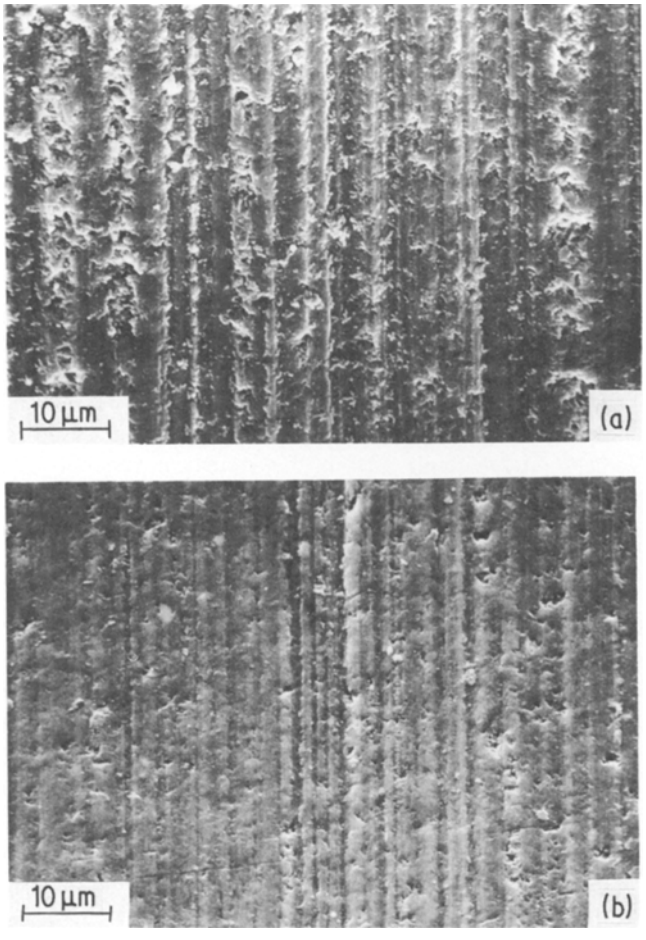

Figure 5 Scanning electron micrographs of the ground surfaces. (a) six, 0.0005 in. (0.013 mm) grinding passes; (b) one, 0.003 in. (0.076 mm) grinding pass.

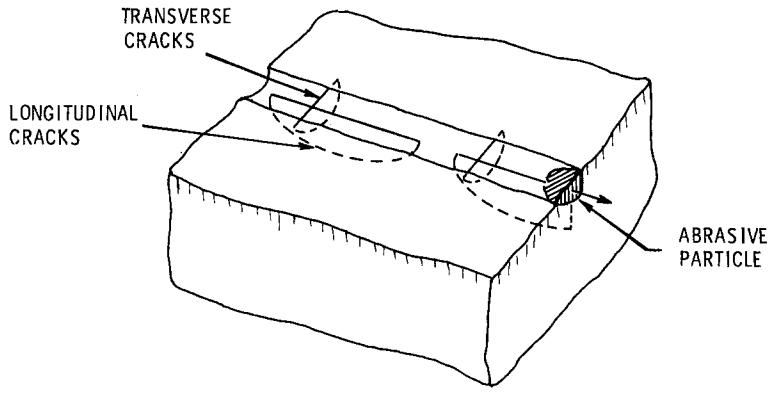

Figure 6 Flaws generated along a typical grinding groove.

in depth and in variability. Comparing the two Weibull moduli indicates that the flexural strength of those beams ground perpendicular to their length dimension ($m = 6.9$) exhibit significantly more variability than the strengths of those specimens ground parallel to their length ($m = 15.2$). Correlating the flexural strength observations to the critical grinding flaws would indicate that those flaws oriented perpendicular to the grinding groove have much less variability in depth than those flaws oriented parallel to the grinding direction. Furthermore, comparison of the scaling parameter σ_0 for the two flaw populations, indicates that the flaws oriented parallel to the grinding direction ($\sigma_0 = 84\,704$ p.s.i., 584 MPa) should be statistically deeper than those flaws oriented transverse to the grinding track ($\sigma_0 = 104\,040$ p.s.i., 718 MPa). The greater variability of the flaws oriented parallel to the grinding groove is thought to arise from their dependence on both the horizontal and vertical grinding forces. The fluctuation of each grinding-force component would then contribute to the total variability of the flaw depth. In contrast, the size of the transverse flaws are dependent only on the vertical grinding force. Thus, only the variability of this single force component should affect the flaw-size variation.

4.3. Multi-pass grinding

The investigations involving multi-pass grinding show it to be a more complex process than single-pass grinding. During each grinding pass, new flaws are introduced into the material's surface while some existing flaws, introduced in previous passes, are removed. This results in a very different situation than that typical of the single-point, single-pass grinding treated by the theory of Conway and Kirchner. The flexural strength data (Table IV) for the beams prepared with six, 0.0005 in. (0.013 mm) grinding passes show no statistical difference between the grinding directions. The equal Weibull moduli and characteristic strengths (Table V) confirm that the size and the variability of the critical flaws oriented parallel and perpendicular to the grinding direction are equal. Additionally, there is no significant difference between the mean flexural strengths of these specimens from that for beams prepared with a single 0.003 in. (0.076 mm) grinding pass parallel to their length dimension, even though the single pass produces a much more severe grinding condition. However, the variability of the flaw depths, as indicated by the Weibull moduli, is different for the single and multi-pass grinding parallel to the specimen's length dimension.

Although the horizontal force was too small to measure during the shallow grinding, it presumably did exist. Thus, the flaw anisotropy theory would predict some deepending of the flaws oriented parallel to the grinding direction. However, if the horizontal-to-vertical load ratio was sufficiently small, only a slight flaw-depth anisotropy would be expected. The resulting difference in flexural strength for the two grinding directions would be undetectable within the statistical variability of the sample.

Residual stresses may play an important role in explaining the absence of a strength anisotropy for the multi-pass grinding condition. The lower grinding forces will produce smaller flaws which might lie entirely within a region of residual tensile stress. A period of stable crack growth might then be encountered during flexural testing as the cracks are propagated along the decreasing residual stress gradient [10]. Therefore, the flaws oriented both parallel and perpendicular to the grinding direction might grow to equal depths before failure. This would produce equal flexural strengths for the two grinding directions.

Elastic/plastic indentation studies of Lawn *et al.* [11] and Uchiyama *et al.* [12] have suggested that the flexural strength for specimens ground perpendicular to their length dimension is given as proportional to the vertical grinding force raised to the $-1/3$ power. The vertical grinding force, recorded in this investigation, increased by a factor of 2.42 when the depth of incursion was increased from 0.0005 in. (0.013 mm) to 0.003 in. (0.076 mm). The theory of Lawn would thus predict a 25% decrease in the flexural strength for those specimens ground with the deeper incursion. This figure is not far from the 18.4% decrease in flexural strength observed in the experimental data (Table IV).

5. Conclusions

5.1. Compliance

There was no detectable effect of the stiffness of the grinding support on the flexural strength of the sialon beams. The Rigidax material was hard and somewhat brittle at room temperature, and therefore possibly did not provide a large enough contrast to the rigid, mechanical clamping arrangement to introduce any observable effects.

5.2. Single-pass grinding

The sialon beams, prepared with a single, 0.003 in. (0.076 mm) grinding pass, exhibited a statistically significant 21% flexural strength anisotropy. An attempt was made to explain this strength difference through a theory developed by Conway and Kirchner. These investigators propose that the horizontal component of the grinding force deepens the flaws which are oriented parallel to the grinding direction, while the flaws oriented perpendicular to the grinding groove are independent of the horizontal force component. The predictions of this model, which was developed for single-point grinding, were complicated by the extension of the theory to multi-point grinding. Material flow at the surface, combined with possible residual stress fields, may have affected the severity of the surface flaws introduced through grinding. The result was that the observed 21% strength anisotropy exceeded the 2.5% difference predicted by the model.

Weibull statistical analysis confirmed that the two orthogonal flaw populations were distinct in their depth and their degree of variability. The flaws oriented along the grinding direction are deeper and exhibit significantly greater variability than those flaws oriented perpendicular to the grinding direction. This was attributed to the dependence of the longitudinal flaws on both components of the grinding force and the dependence of the transverse flaws on only one component of the grinding force.

5.3. Multi-pass grinding

Preparing the sialon beams with six grinding passes of 0.0005 in. (0.013 mm) resulted in an equal flexural strength for both grinding directions. Furthermore, the variability of the flexural strengths for the two grinding directions is the same, as evidenced by the Weibull moduli.

The lack of observed sensitivity of the flexural strength to the grinding direction was attributed to several possible factors. The horizontal-to-vertical load ratio during grinding may have been sufficiently low such that the strength anisotropy predicted by Conway and Kirchner was undetectable within the variability of the experimental data. Also, the lower grinding forces may have introduced flaws which lie entirely within a region featuring a decreasing residual stress gradient, thereby allowing stable crack growth to occur before failure. Furthermore, the complexities of multi-pass grinding may alter the depths and the variability of the flaws found in the ground surface. During each successive grinding pass, new surface flaws are introduced, some existing flaws are removed, and some of the existing flaws are propagated to greater depths.

6. Future work

Further investigation is required to isolate and explain the mechanisms present during single-pass and multi-pass grinding. Ground specimens will be back-fractured in such a manner as to maintain the ground surface in compression. Scanning electron microscopy will then be used to observe and measure the grinding flaws oriented both parallel and perpendicular to the grinding direction. This information will then be correlated with Conway and Kirchner's flaw-anisotropy model. Additionally, this technique will determine if such a depth difference does exist between the orthogonal flaws for the 0.0005 in. (0.013 mm) grinding depth.

An improvement of the grinding-force measurement system will allow for more accurate peak-load data to be obtained. Filtering the signal to eliminate the effects of spurious vibrations will

allow the small horizontal grinding forces to be measured at the shallow depths of incursion. From this information, reliable horizontal-to-vertical load ratios will be determined to aid further in the correlation of the experimental data to the analytical model.

Acknowledgements

The authors wish to thank the Philip M. McKenna Foundation for their support of one of the investigators (MWH).

References

1. P. HARTLEY, *Engineering* **220** (1980) 1010.
2. T. E. EASLER, T. A. COUNTERMINE, R. E. TRESSLER and R. C. BRADT, in "The Science of Ceramic Machining and Surface Finishing II", National Bureau of Standards Special Pub. 562, edited by B. J. Hockey and R. W. Rice (National Bureau of Standards, Washington DC, 1979) p. 455.
3. C. A. ANDERSSON and R. J. BRATTON, in "The Science of Ceramic Machining and Surface Finishing II", National Bureau of Standards Special Pub. 562, edited by B. J. Hockey and R. W. Rice (National Bureau of Standards, Washington DC, 1979) p. 463.
4. C. CM. WU and K. R. McKINNEY, in "The Science of Ceramic Machining and Surface Finishing II", National Bureau of Standards Special Pub. 562, edited by B. J. Hockey and R. W. Rice (National Bureau of Standards, Washington DC, 1979) p. 477.
5. J. J. MECHOLSKY Jr, S. W. FREIMAN and R. W. RICE, *J. Amer. Ceram. Soc.* **60** (1977) 114.
6. A. BROESE VAN GROENOU and R. BREHM, in "The Science of Ceramic Machining and Surface Finishing II", National Bureau of Standards Special Pub. 562, edited by B. J. Hockey and R. W. Rice (National Bureau of Standards, Washington DC, 1979) p. 61.
7. "1983 Annual Book of ASTM Standards", B 406-76 (Reapproved 1982), Sect. 2, Vol. 5.
8. R. W. RICE and J. M. MECHOLSKY Jr, in "The Science of Ceramic Machining and Surface Finishing II", National Bureau of Standards Special Pub. 562, edited by B. J. Hockey and R. W. Rice (National Bureau of Standards, Washington DC, 1979) p. 351.
9. J. C. CONWAY Jr and H. P. KIRCHNER, *J. Mater. Sci.* **15** (1980) 2879.
10. H. P. KIRCHNER and E. D. ISAACSON, *J. Amer. Ceram. Soc.* **65** (1982) 55.
11. B. R. LAWN, A. G. EVANS and D. B. MARSHALL, *ibid.* **63** (1980) 574.
12. T. UCHIYAMA, D. B. MARSHALL and A. G. EVANS, in "Micro and Macro Mechanics of Fracture in Ceramics", Interim Report to Office of Naval Research, Contract No.: N00014-81-K-0362 (1982) p. 142.

Received 6 March
and accepted 27 March 1984